33RD CONGRESS
OF THE INTERNATIONAL COUNCIL
OF THE AERONAUTICAL SCIENCES
STOCKHOLM, SWEDEN, 4-9 SEPTEMBER, 2022

FATIGUE DAMAGE MODEL OF HIGH TEMPERATURE POLYMER COMPOSITES IN AERO-ENGINES

Vivek Richards Pakkam Gabriel, Patrik Fernberg.

Department of Engineering Sciences and Mathematics, Luleå University of Technology, SE-97187 Luleå, Sweden.

Abstract

High Temperature Polymer Cross-ply (HTPC) laminate specimens are subjected to tension-tension fatigue loading at 3 different maximum stress levels at room temperature. Transverse cracking in 90° layer in the cross-ply laminate upon fatigue tests is analyzed. Based on probabilistic approach, using Weibull distribution, a prediction model for the increase in number of transverse cracks upon fatigue loading at different stress levels is developed. The predicted crack density (number of cracks per unit length) development shows good agreement with the test results for fatigue at the higher stress levels considered. A slight overprediction is observed at lowest stress level.

Keywords: High temperature polymer composite, fatigue loading, Weibull distribution, transverse cracks.

1. Introduction

Composite materials made from fibers reinforced by polymer matrix are attractive candidates for lightweight engineering applications. They provide advantages such as low density, high stiffness and strength to weight ratio etc. The structures are usually manufactured by autoclave curing of prepregs, resin transfer molding (RTM) or Vacuum Assisted RTM (VARTM) to produce laminates where plies with different fiber orientation are stacked to tailor the desired thermo-elastic constants. In aerospace, usage of composite laminate is increasing and currently making up more than 50% in weight of some modern aircrafts [1,2]. Recent developments include increased use of composites in parts like fan blades, casing of low compressor region in aero-engines [3] where the service temperature may vary from ambient temperature to around 100℃. One new challenge would be to push the limit of composite structures towards parts with higher service temperature e.g., where maximum temperature could reach around 150℃ - 200℃. Such composite structures will consequently be exposed to a) long term exposures to elevated temperatures, b) thermal cycling combined with moisture absorption and desorption and c) mechanical fatigue loading at service. This complex combination of hygro-thermo-mechanical load may influence the material in terms of its ability to withstand loads without introducing damage as well as influencing the rate at which damage accumulate in the composite material. Accumulation of damage leads to stiffness degradation in the material.

Progressive damage models are consequently needed to predict the damage accumulation and its associated stiffness degradation at various loading conditions. The work presented is based on previous and current developments of a damage prediction model using Weibull failure stress distribution [4,5]. The damage mentioned here refers to increase in number of transverse cracks when subjecting composite laminates to quasi-static tensile loading and tension-tension fatigue loading at room temperature (RT). Using Weibull distribution, the failure stress is distributed to all elements in 90° layer along the transverse direction. Then the crack density can be determined by use of stresses obtained from Classical Laminate Theory (CLT) and from the probability of failure of elements. Detailed explanations are given in section 2, 3 and 6. Initial validation was on glass fiber reinforced epoxy composites. Here, the fatigue damage mechanism of high temperature polymer composite material system is analyzed and the corresponding fatigue damage model for transverse crack prediction under tension-tension fatigue loading at RT is developed and investigated.

2. Crack development under fatigue loading

Composite laminates when subjected to mechanical tensile loading, transverse/intralaminar crack usually develops in the off-axis layer of the composite laminate with respect to the loading direction. The cracks in Fig. 1a are in Glass Fiber reinforced in Epoxy (GF/EP) prepreg cross-ply laminate and Fig. 1b are in carbon fiber UniDirectional (UD) fabric reinforced in high temperature polymer. The cracks are in 90° layer of the composite laminate here in this work. This is because, the stiffness and the strength of the 90° layer is lower than in the loading direction (which is 0° layer here) [6]. The cause of cracks in an off-axis layer is usually the in-plane transverse and shear stress [7,8]. Since the off-axis layer is 90° for cross-ply laminates, the shear stress can be neglected in the current work. The cracks in addition to extending the whole thickness of the 90° layer, also runs along the fibers to extend as tunnels through the width of a specimen, see Fig. 2a, with the crack face plane perpendicular to the x-y plane as illustrated in Fig. 2b. Often the increase in number of cracks is presented as crack density (number of cracks per unit length or inversely proportional to the distance between two existing cracks, '$2l$'). The crack density growth also results in degradation of stiffness of the composite laminate [9,10].

Using Linear Elastic Fracture Mechanics (LEFM) [11], the crack development can be analyzed using the concept of Energy Release Rate (ERR). Based on the earlier discussion in this section, the crack development can be divided into two stages: 1) Crack initiation, 2) Crack propagation.

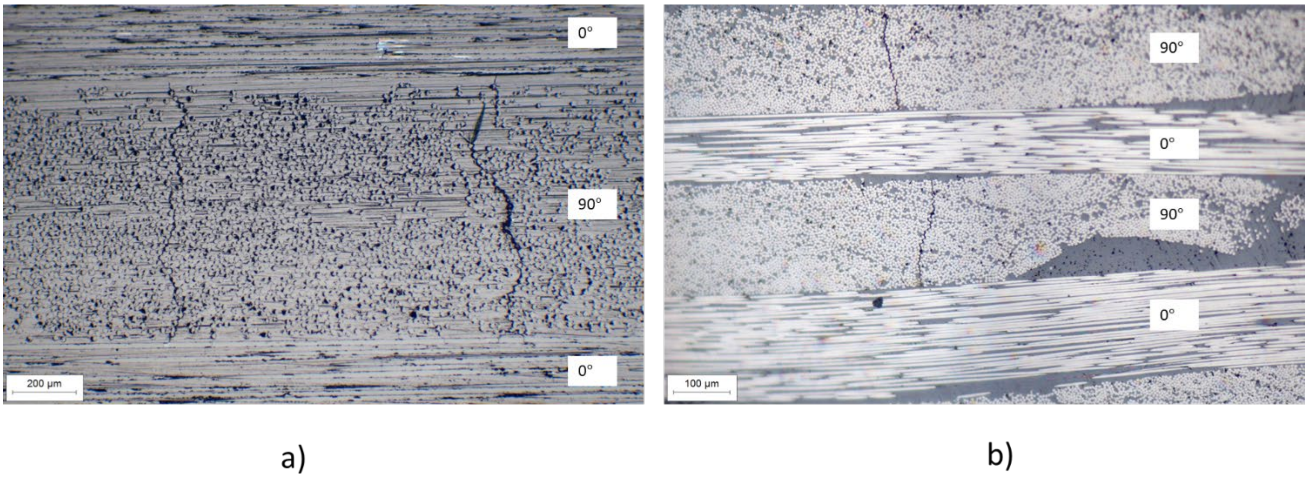

Figure 1: Microscopic edge view of a) GF/EP [0/90]s b) carbon fiber UD fabric reinforced in high temperature polymer cross-ply laminate [0/90/0/90$_{0.5}$]s.

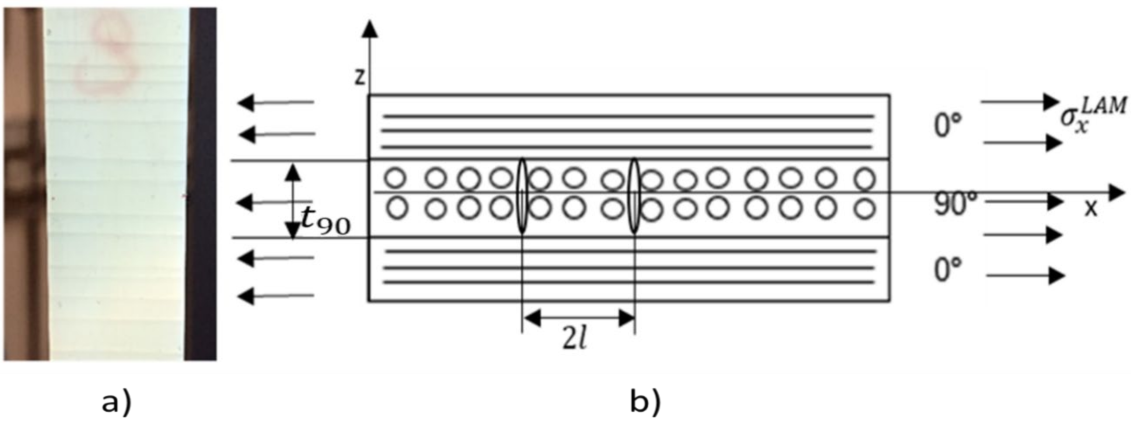

Figure 2: a) Surface view of GF/EP, dark visible lines are the tunneling cracks b) Schematic view of the [0/90/0] with 2 cracks separated by distance of $2l$ and stress (σ_x^{LAM}) applied along 0° layer.

2.1. Crack Initiation

A transverse crack initiates from fiber/matrix debonding [9,12], matrix cracking [13,14], defects in 90° layer from manufacturing or specimen preparation coalescence together with the initiated crack to grow in thickness direction to a critical size. As the size of the crack grows, ERR increases. Once it attains the critical size, the ERR reaches the sufficient level for the crack to grow unstably in the thickness direction [15] until it covers the whole thickness of 90° layer. Then the crack gets arrested at the interface between two different layers. The transverse stress required to initiate the crack into critical size is the failure initiation transverse stress. Assuming a homogenized 90° layer, this stress can be calculated using Classical Laminate Theory (CLT) as the sum of thermal stress (developed in the 90° layer during the cool down from manufacturing temperature to the use temperature) and applied mechanical stress.

2.2. Crack Propagation

The crack propagates along the fiber direction in 90° layer and forms tunnel like shape. The crack growth along fibers depends on the available ERR from the crack size, which also depends on the thickness of 90° layer. The dependence of the transverse stress required for the propagation along fibers, with the thickness of the 90° layer t_{90} is given by $1/\sqrt{t_{90}}$ [10,16]. Thus, the stress required for crack growth along fibers is higher in thin 90° layers compared to thick layer. That is for the thick 90° layer used here; the stress required for crack propagation along fibers is lower than what is needed for the crack initiation. Consequently, the crack propagates instantly through width of the specimen forming a tunneling crack once a crack is initiated. Hence, the failure initiation stress becomes the failure stress for a certain position in 90° layer. Also due to the non-uniformity in distribution of the fiber clusters and/or the defect regions in 90° layer, different failure stress is consequently required in different positions, which is defined using Weibull distribution in the section 3.

From experiments in fatigue, it has been observed that certain number of cycles are required to initiate a crack and certain number of cycles for crack propagation along fibers in a position in 90° layer under stress-controlled fatigue loading. This fatigue effect has been reflected in model as reduction in crack resistance in 90° layer upon cyclic loading and the failure stress in the positions decreases upon cyclic loading. Thus, different number of cycles are required for crack initiation at different positions in the 90° layer. In case of crack propagation along fibers, it has been assumed that the crack growth, follows Paris law with respect to ERR changes in one cyclic load [7], and it has been confirmed that crack growth rate along fibers has power function dependence on the total ERR. Thus, the ERR available for the crack propagation along the fibers at the same stress is larger in thick plies and the crack propagates much faster. Also, from the experiments it has been observed that most of the cracks are tunneling cracks, suggesting that number of cycles taken for propagation along fibers are lesser than it has taken for the crack initiation. So, it can be assumed that the number of cycles required to develop a fully grown crack is same as the number of cycles required to initiate a crack at a position in 90° layer.

3. Weibull Distribution

From [17,18] it has been observed that at a given load one crack appears and the load has to be increased to have new cracks. Thus, the distribution of fiber clusters and/or the defects in 90° layer follows a statistical distribution, so is the failure stress and different positions in 90° layer has different cracking resistance. Assuming the distribution of the failure stress as a chain of weak links, each with different failure stress, it can be defined using Weibull distribution.

Based on Weibull distribution, the probability of failure of the elements of length l_{el} can be determined when the applied thermo-mechanical transverse increases from 0 to σ_T. For quasi-static tensile loading, the probability of failure P_f can be defined using Weibull shape parameter m and scale parameter σ_0 for a reference element length l_{ref}. P_f can also be expressed in terms of crack density ρ over the maximum possible crack density ρ_{max} in the 90° layer. Assuming l_{ref} equal to t_{90} from [8] and the determining P_f for an $l_{el} = t_{90}$, then the P_f can be expressed as

$$P_f = \frac{\rho}{\rho_{max}} = 1 - exp\left(-\left(\frac{\sigma_T}{\sigma_0}\right)^m\right). \tag{1}$$

Under cyclic loading, since the resistance to failure in each position of 90° layer decreases upon every cyclic load, the failure stress also decreases. In [19], to incorporate this fatigue effect in the Weibull distribution it is assumed that the decrease in failure resistance can be interpreted as monotonous decrease of the scale parameter with respect to the number of fatigue cycles and maximum stress in 90° layer. This can be expressed in simple power function, and it is given by,

$$\sigma_0 = A \cdot N^{-\alpha} \left(\frac{\sigma_T^{fat}}{B}\right)^{-\gamma}, \quad \gamma \geq 0, \ \alpha \geq 0, \ N \gg 1, \tag{2}$$

where A, α, γ and B are unknown material constants and σ_T^{fat} is the fatigue stress in 90° layer. Substituting (2) in (1) gives

$$\frac{\rho}{\rho_{max}} = 1 - exp\left[-N^{\alpha \cdot m}\left[\left(\frac{\sigma_T^{fat}}{B}\right)^{\gamma} \frac{\sigma_T}{A}\right]^{m}\right]. \tag{3}$$

For pure cyclic loading it can be assumed that $\sigma_T = \sigma_T^{fat}$, and without losing generality, it can be assumed that $A = B = \sigma^*$. Then (3) becomes,

$$\frac{\rho}{\rho_{max}} = 1 - exp\left[-N^{n}\left[\frac{\sigma_T^{fat}}{\sigma^*}\right]^{m^*}\right], \tag{4}$$

where $m^* = m(1+\gamma)$ is the shape parameter, $n = \alpha \cdot m$ is the fatigue parameter and σ^* is the scale parameter for the cyclic loading. For simple data reduction methodology, it can be assumed that $\sigma_T^{fat} = \sigma_{T0}^{fat}$ where σ_{T0}^{fat} is the fatigue stress in undamaged 90° layer. In log-log axis of (4) as in,

$$ln\left(-ln\left(1 - \frac{\rho}{\rho_{max}}\right)\right) = n \, ln \, N + m \, ln \frac{\sigma_{T0}^{fat}}{\sigma^*}, \tag{5}$$

the data reduction is performed, and Weibull parameters are determined.

4. Materials and Experimental Description

Carbon Fiber (CF) made of UD fabric with sparsely woven yarns in both warp and weft direction reinforced in high temperature polymer or Temperature Resistant Polymer (TRP), UD and cross-ply laminates, $[0/90/0/90_{0.5}]_s$, were manufactured by RTM. The thermo-mechanical elastic constants of the laminate are given in table 1. Elastic constants for CF/TRP were obtained from experiments on UD laminate. Table 1 also have difference between manufacturing temperature and RT, thickness of 90° layer t_{90} and difference between coefficient of thermal expansions $\Delta\alpha$. $\Delta\alpha$ was estimated from the elastic ply properties and from literature data of the constituent materials. From image analysis, the volume fraction of fibers V_f were estimated to be 57%. GF/EP cross-ply laminate from [5,19] was used here for comparison with the CF/TRP specimens for the prediction of transverse cracks. Also, elastic constants of GF/EP are given in table 1.

Table 1: Elastic and geometric properties used for CLT analysis

Material	E_1 (GPa)	E_2 (GPa)	ν_{12}	ΔT (°C)	t_{90} (mm)	$\Delta\alpha$ (1/°C)
GF/EP	37.86	9.28	0.28	-95	0.75	$2.39e^{-5}$
CF/TRP	131.09	9.83	0.27	-227	0.17	$3.25e^{-5}$

Specimens (from manufactured cross-ply laminates) edges were grinded and polished to reduce edge defects and to enable optical observation of the damage state in 90° layer. The average dimensions of the tested specimens were 180.00 x 13.50 x 1.15 mm^3. The distance between the tabs or the grips were 100mm. Upon observing the CF/TRP manufactured specimens' edges, it was found that although laminate had a high V_f, individual layers retained their bundle structure, with warp yarns prominently located between bundles within resin rich regions in 90° layer, as marked in red circles in

Fig. 3a. Also, warp yarns located between fiber bundles of 2 different layers in few places. Several debonds between the yarn fibers and matrix region were observed, which acted as weak regions to initiate a crack in the 90° layer upon fatigue loading. Very few transverse cracks induced from cooling down from manufacturing temperature to room temperature in the 90° layer was observed. The average number of bundles and average length of the compacted bundles along transverse direction (within 50mm gauge length) in 90° layer was 18 and 2.4mm respectively.

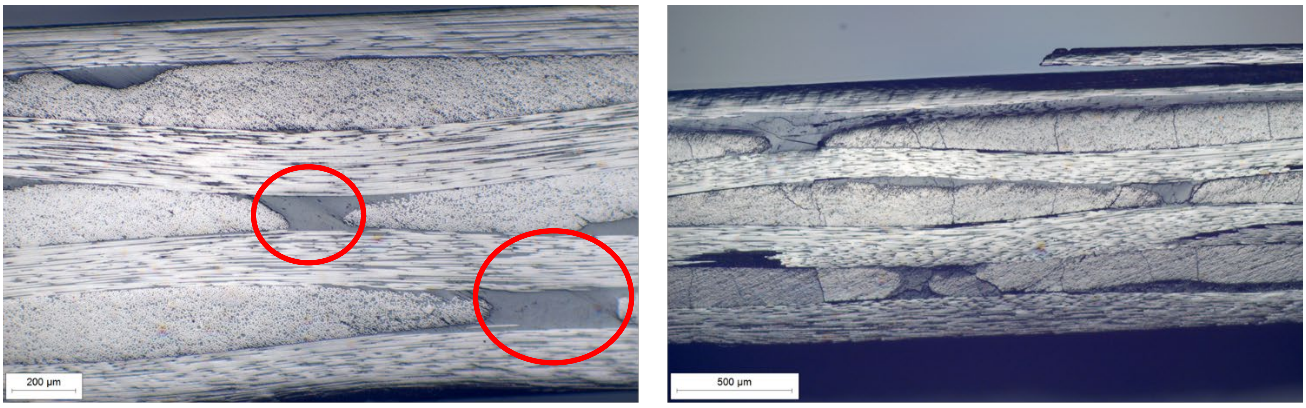

a) b)

Figure 3: Optical edge view of a) undamaged as manufactured laminate; b) laminate after failure.

Stress controlled tension-tension fatigue tests were performed on an INSTRON ElectroPuls^{TM} E10000 tension-torsion testing machine with frequency 5 Hz (for CF/TRP specimens) and 6 Hz (for GF/EP specimens) and stress ratio R=0.1 at room temperature (RT). CF/TRP specimens were tested at three maximum stress levels and its corresponding thermo-mechanical transverse stresses in 90° layer was 114.75 MPa, 124.52 MPa and 134.29 MPa. Similarly, GF/EP specimens were tested at three different maximum stress levels and its corresponding thermo-mechanical transverse stresses in 90° layer was 52 MPa, 61.1 MPa and 70.27 MPa. Thermal stresses in 90° layer at RT were 66.42 MPa for CF/TRP specimens and 15.24 MPa for GF/EP specimens. Fatigue tests were performed to certain number of fatigue cycles to introduce cracks at each stress level. Before and after each step of fatigue cycles, the stiffness was determined from strain loading-unloading step at a constant displacement rate of 2mm/min using extensometer with gauge length of 50mm. The crack density was also determined between every fatigue step. In case of GF/EP, the cracks were quantified using a light illuminated from backside of the specimen, where the cracks appear as dark visible lines, see Fig. 2a. Also, the cracks were quantified on the edges under optical microscope or using Struers Repliset (especially for CF/TRP specimens) within the same 50 mm gauge length used for stiffness measurements.

5. Experimental Results

The crack density versus the number of cyclic loads were given in Fig. 4a-c for GF/EP specimens tested at 3 stress levels and Fig. 4d-f for CF/TRP specimens tested at 3 stress levels and their corresponding stress in 90° layers is given in the graph title. The results of the GF/EP specimens have already been analyzed by the authors in [5,19].

In Fig. 4d-f, the crack density mentioned was from the average crack density of all 90° layers on both edges of the specimens. From the first fatigue cycle it can be observed that specimens had high crack density and continued increasing steadily with the number of cycles. A general observation is that, as the fatigue stress level increases, the crack density from first cycle increases and this tendency continued in the growth of crack density as the number of cycles increases. At initial fatigue cycles in all stress levels, the number of cracks observed within fiber bundles and vicinity of warp yarn regions were almost the same. As the number of cycles increased, the relative crack density growth rate within bundles was higher than in the warp yarn regions. Later, delamination at crack tips between different layers started growing with increase in number of cycles. Unlike GF/EP specimens, the CF/TRP specimens had rapid crack density growth upon cyclic loading, until final failure. The specimens failed even before reaching the characteristic damage state [8], in fact, it failed around $P_f = 0.5$. Also, the specimens tested at higher stress levels failed earlier around 50000 to 100000th cycle. The failure mode mentioned here is the complete debonding or the large delamination of bundles in 0° layer with fiber breakage at edge of the specimens, see Fig. 3b.

6. Weibull Parameter Determination Methodology

The testing methodology involves in detailed stress-controlled fatigue test at one stress level and obtain all data points of crack density within non-interactive crack density region $0.05 < P_f < 0.3$ [4] with respect to the number of cycles. In addition to that, fatigue test at a higher stress level is to be performed to obtain one data point that is crack density within the non-interactive crack density region. Non-interactive crack density region is the region where cracks are far apart and the stress between the cracks are almost equal to the far field or CLT transverse stress. In this fatigue model based on Weibull distribution, the Weibull parameters are assumed to be same for all the fatigue stress levels.

In CF/TRP specimens, the crack density from the first cycles at 124.52 MPa stress level were higher with an average crack density of 0.47 cr/mm. As a compromise between theoretical and practical requirements, the data points used were between the 0.73 and 2.49 cr/mm, corresponding to $0.12 < P_f < 0.41$. Based on the Weibull parameter determination methodology developed in [19], the Weibull parameters for CF/TRP and GF/EP material system were determined and given in table 2.

Table 2: Weibull parameters obtained for GF/EP and CF/TRP

Material	**Test method**	**Fatigue parameter n**	**Shape parameter m^***	**Scale parameter σ^* (MPa)**
GF/EP	All data points from 61.1 MPa fatigue test and one data point at 70.27 MPa (from ref [19])	0.72	13.94	113.57
CF/TRP	All data points from 124.52 MPa fatigue test and one data point at 134.29 MPa	0.18	2.83	314.18

7. Results and Discussions

Using the Weibull parameters in table 2 for the respective material system, the crack density based on probabilistic approach is predicted versus the number of cycles at different stress levels. In GF/EP obtained in previous research and shown here for reference, see Fig. 4a-c, the probabilistic predicted results were in good agreement with the test results of all stress levels in non-interactive or low crack density region. In fact, it is the region where the Weibull parameters were determined. As expected, beyond that region, the cracks start to interact (interactive or high crack density region), and the creation of new cracks depend on the stress distribution between the existing cracks. Thus, the authors suggested novel stress distribution model in [4,5] and using Monte Carlo method the crack density at interactive crack density region has been successfully predicted.

From Fig. 4d-f, the crack density prediction for CF/TRP using the Weibull parameters in table 2, were in rather good agreement with test results for most stress levels although for the lowest (114.75 MPa) an overprediction is noticed. Despite the shortcomings, the developed prediction methodology was found to predict the crack density with good agreement, particularly at higher stress levels.

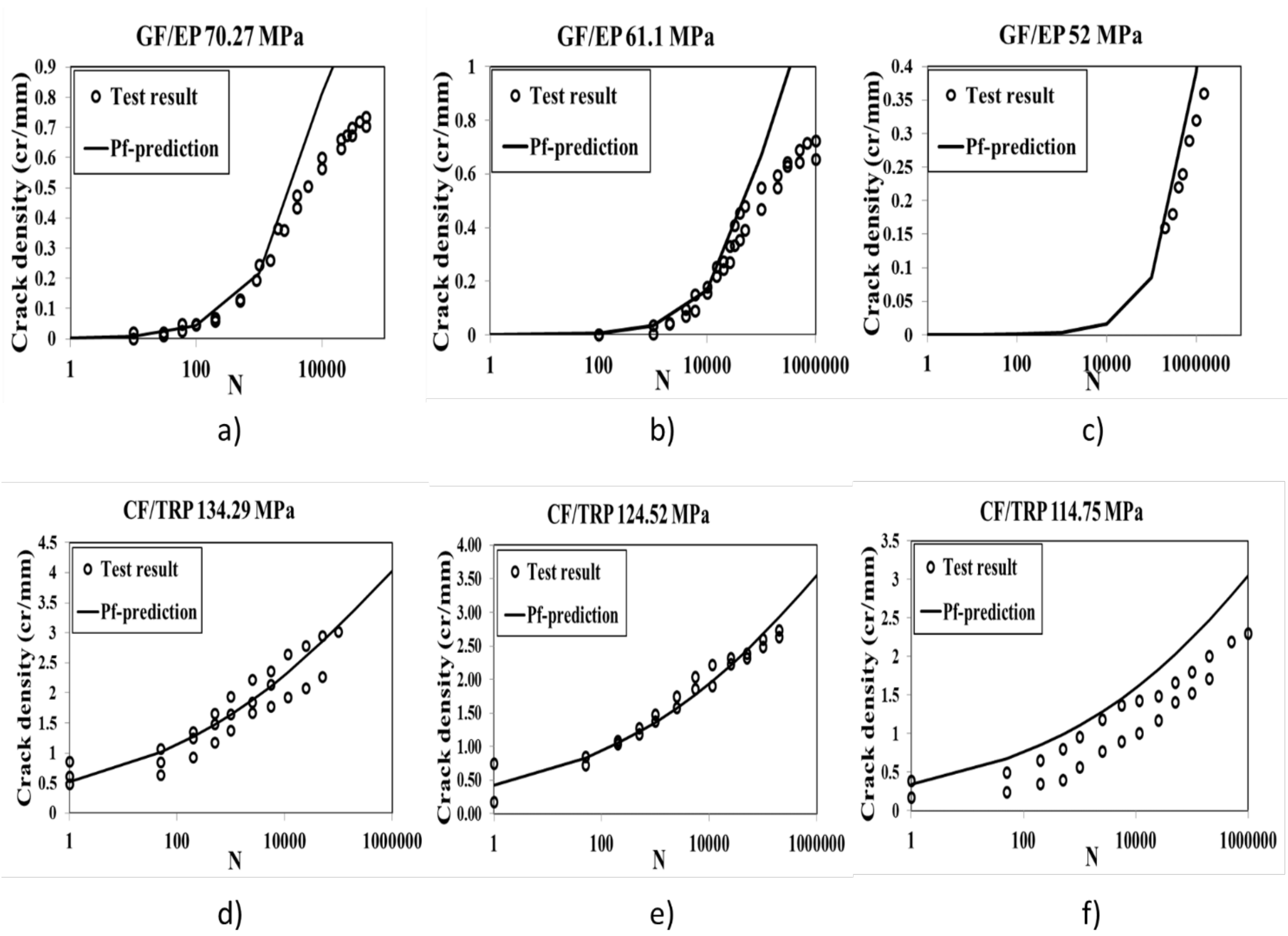

Figure 4: Crack density (cr/mm) versus number of fatigue cycles; (a-c) for GF/EP from [19] and (d-f) for CF/TRP; with thermo-mechanical transverse stress in 90° layer is mentioned in title; Black circles are test data and black solid line is probabilistic ‘P_f’ prediction based on Weibull parameters given in table 2.

8. Conclusion

Transverse cracking upon tension-tension fatigue loading in GF/EP and CF/TRP cross-ply laminates at several stress levels obtained in this work and in previous, were compared, analyzed and predicted using a probabilistic approach. Upon fatigue loading of the specimens, the crack density growth tends to increase as the maximum stress level increases. Also, the crack density growth in CF/TRP specimens were rapid until final failure. Assuming the distribution of the fiber clusters and warp yarns (in case of CF/TRP specimens) in 90° layer follows Weibull distribution, the probability of failure of the elements in 90° layer was determined. Using the developed parameter determination methodology and determined Weibull parameters, the crack density growth was predicted with good agreement for different stress levels with respect to number of fatigue cycles in non-interactive crack density region for GF/EP and in whole crack density region at higher stress levels in CF/TRP specimens.

9. Acknowledgement

This work has been performed within the Swedish Aeronautical Research Program (NFFP7), project 2019- 02777. The authors would like to thank Miguel Moldes Carballal, for support with the experimental characterization of CF/TRP samples and Prof. Janis Varna and Dr Mohamed Loukil for valuable contributions to methodology development.

10. Contact Author Email Address

mailto: patrik.fernberg@ltu.se

11. Copyright Statement

References

[1] Fortune business insights, https://www.fortunebusinessinsights.com/composites-market-102295, (Accessed online 03/05/2022)

[2] Giurgiutiu V. Chapter 1 – Introduction, Structural Health Monitoring of Aerospace Composites, 1-23, 2016.

[3] Marsh G, “Aero engines lose weight thanks to composites”, *Reinforced Plastics*, Vol. 56, No. 6, 32-35, 2015.

[4] Gabriel VRP, Loukil MS and Varna J. Analysis of intralaminar cracking in 90-plies of GF/EP laminates with distributed ply strength, *Journal of Composite Materials*, Vol. 55, Issue 26, 3925-3942, 2021.

[5] Gabriel VRP, Loukil MS and Varna J. Intralaminar cracking during cyclic loading in laminates with distributed failure stress in 90-plies, *International Journal of Fatigue*, Vol. 161, 106909, August 2022.

[6] Nairn JA. Matrix microcracking in composites, In: Kelly A, Zweben C, Talreja R, Manson J-A, editors. Comprehensive Composite Materials, *Polymer Matrix Composite*, Amsterdam: Elsevier, 2: 403-432, 2000.

[7] Quaresimin M, Carraro PA, Mikkelsen LP, Lucato N, Vivian L, Brøndsted P, Sørensen BF, Varna J and Talreja R. Damage evolution under cyclic multiaxial stress state: A comparative analysis between glass/epoxy laminates and tubes, *Composites Part B: Engineering*, Vol. 61, 282-290, 2014.

[8] Reifsnider KL and Jamison R. Fracture of fatigue-loaded composite laminates, *International Journal of Fatigue*, Vol. 4, Issue 4, 187-197, 1982.

[9] París F, Cano J and Varna J. The fiber-matrix interface crack – a numerical analysis using boundary elements, *International Journal of Fracture*, Vol. 82, Issue 1, 11-29, 1990.

[10] Parvizi A and Bailey JE. On multiple transverse cracking in glass fiber epoxy cross-ply laminates, *Journal of Material Science*, Vol. 13, Issue 10, 2131-2136, 1978.

[11] Broek D, *Elementary engineering fracture mechanics*, Martinus Nijhoff Publishers, 1982.

[12] Zhuang L, Pupurs A, Varna J, Talreja R and Ayadi Z. Effects of inter-fiber spacing on fiber-matrix debond crack growth in unidirectional composites under transverse loading, *Composite Part A*, Vol. 109, 463-471, 2018.

[13] Zhuang L, Talreja R and Varna J. Transverse crack formation in unidirectional composites by linking of fibre/matrix debond cracks, *Composites Part A*, Vol. 107, 294-303, 2018.

[14] Herráez M, Mora D, Naya F, Lopes CS, González C and LLorca J. Transverse cracking of cross-ply laminates: A computational micromechanics perspective, *Composites Science and Technology*, Vol. 110, 196-204, 2015.

[15] Paris F, Blazquez A, McCartney LN and Mantic V. Characterization and evolution of matrix and interface related damage in [0/90]s laminates under tension, Part I: Numerical predictions, *Composites Science and Technology*, Vol. 70, 1168-1175, 2010.

[16] Dvorak GJ and Laws N. Analysis of progressive matrix cracking in composite laminates II. First ply failure, *Journal of Composite Materials*, Vol. 21, Issue 4, 309-329, 1987.

[17] Peters PWM. The strength distribution of 90° plies in 0/90/0 Graphite-Epoxy laminates, *Journal of Composite Materials*, Vol. 18, Issue 6, 545-556, 1984.

[18] Joffe R and Varna J. Analytical modeling of stiffness reduction in symmetric and balanced laminates due to cracks in 90° layers, *Composites Science and Technology*, Vol. 59, Issue 11, 1641-1652, 1999.

[19] Vivek Richards Pakkam Gabriel, Mohamed Sahbi Loukil, Patrik Fernberg and Janis Varna. Methodology for transverse cracking simulation in 90 plies of composite laminate under fatigue loading, *20th European Conference on Composite Materials (ECCM20)*, submitted, 26-30 June 2022.